

ARTICLE

Practical Considerations for Implementing Adaptive Acoustic Noise Cancellation in Commercial Earbuds

Agustinus Oey[®]

VizWave Inc., Seongnam, 13595, Korea

ABSTRACT

Active noise cancellation has become a prominent feature in contemporary in-ear personal audio devices. However, due to constraints related to component arrangement, power consumption, and manufacturing costs, most commercial products utilize fixed-type controller systems as the basis for their active noise control algorithms. These systems offer robust performance and a straightforward structure, which is achievable with cost-effective digital signal processors. Nonetheless, a major drawback of fixed-type controllers is their inability to adapt to changes in acoustic transfer paths, such as variations in earpiece fitting conditions. Therefore, adaptive-type active noise control systems that employ adaptive digital filters are considered as the alternative. To address the increasing system complexity, design concepts and implementation strategies are discussed with respect to actual hardware limitations. To illustrate these considerations, a case study showcasing the implementation of a filtered-x least mean square-based active noise control algorithm is presented. A commercial evaluation board accommodating a low-cost, fixed-point digital signal processor is used to simplify operation and provide programming access. The earbuds are obtained from a commercial product designed for noise cancellation. This study underscores the importance of addressing hardware constraints when implementing adaptive active noise cancellation, providing valuable insights for real-world applications.

Keywords: Active noise cancellation; Adaptive filter; DSP implementation

1. Introduction

The use of the active noise control (ANC) method to reduce ambient noise in the earbuds has achieved significant commercial success, demonstrating the

*CORRESPONDING AUTHOR:

Agustinus Oey, VizWave Inc., Seongnam, 13595, Korea; Email: oeaugust@vizwave.net

ARTICLE INFO

Received: 7 October 2023 | Revised: 26 October 2023 | Accepted: 30 October 2023 | Published Online: 6 November 2023

DOI: <https://doi.org/10.30564/jeis.v5i2.5998>

CITATION

Oey, A., 2023. Practical Considerations for Implementing Adaptive Acoustic Noise Cancellation in Commercial Earbuds. *Journal of Electronic & Information Systems*. 5(2): 25-34. DOI: <https://doi.org/10.30564/jeis.v5i2.5998>

COPYRIGHT

Copyright © 2023 by the author(s). Published by Bilingual Publishing Group. This is an open access article under the Creative Commons Attribution-NonCommercial 4.0 International (CC BY-NC 4.0) License. (<https://creativecommons.org/licenses/by-nc/4.0/>).

effectiveness of the method in the frequency range where the spatial control region is small in comparison to the wavelength. The problem itself can be simply considered as a one-dimensional problem—that is, the cancellation of plane waves. However, incorporating ANC into earbuds presents specific challenges, primarily due to the compact form factor essential for earbud design. These challenges include fitting all the required components into a tiny enclosure and dealing with tight spacing between the sensor and actuator, which limits the response time of an ANC system. This necessitates low-latency audio processing devices and computationally efficient control algorithms. Achieving significant noise reduction across a broad bandwidth depends on minimizing latency^[1].

Another important factor to be considered for a well-performing ANC system is the variation in acoustic leakage within the acoustic control region. This variability is mainly associated with user preferences for diverse earbud fit conditions to ensure comfortable wear. On some occasions, the fit may also loosen as the user moves. Obviously, a stronger anti-noise signal is required to compensate for the increase in acoustic leakage. However, even a minor alteration in the leakage causes variability in the way ambient noise propagates into the ear. This introduces uncertainty in how a controller would respond. Consequently, controller stability and noise reduction performance must be assured within the assumed perturbed range.

One of the earliest approaches proposed to address uncertainty in active headsets is the utilization of a robust controller^[2]. This method employs an algorithm based on the two Riccati equations to determine appropriate parameters for a controller with guaranteed operating margins. The resulting controller is implemented using operational amplifier circuitry. Another noteworthy alternative approach involves employing a set of stable feedback controllers with various preset gains^[3]. In response to specific fitness conditions, a comparator switches to the appropriate operational controller. These studies shed light on the idea that a certain degree of controller

adaptiveness is generally necessary to accommodate varying acoustic environments.

In the field of ANC applications, adaptive controllers incorporating digital filters have gained popularity for their ability to efficiently adapt to dynamic and complex acoustic environments. However, practical implementation within earbuds presents challenges due to the limited choice of computing hardware, which compromises the system's ability to perform complex calculations. High-performing processor is essential for executing sophisticated control algorithms requiring intensive and intricate digital filtering tasks^[4].

Achieving effective ANC in resource-constrained earbuds demands a careful balance of design factors to ensure satisfactory noise cancellation performance. This article investigates practical considerations for implementing adaptive filters in noise cancellation, specifically utilizing a low-cost digital signal processor (DSP) suitable for earbud integration. The adaptive controller employs the well-known filtered-x least mean square algorithm (FxLMS). Details about the specifications of the speakers and microphone, as well as their spatial arrangement, are derived from a popular commercial earbud product. The overall configurations are determined based on computational resources and the functional features available within the chosen DSP. Finally, the article presents experimentation using broadband random noise to validate the proposed approach.

2. Adaptive noise control system

Figure 1(a) illustrates a simplified ANC system within earbuds. The interface unit performs signal conditioning and audio codec, as well as signal mixing and amplification. To reduce ambient noise, typically assumed to be random and broadband, a feed-forward controller is commonly adopted. This setup involves one speaker to generate the anti-noise and two microphones: one positioned upstream and another downstream to measure the reference input, $x(n)$, and the noise residue, $e(n)$, respectively. When the speaker and error microphone are placed within a sealed enclosure, two propagation paths must be con-

sidered. The first is referred to as the primary path, $P(z)$, through which noise travels from the reference microphone to the error microphone. This path is purely acoustical in nature. The other is the secondary path, $S(z)$, which exists between the controller's output and input ports. It is a propagation medium that comprises both electrical components within the circuitry of the signal interface unit, speaker, and error microphone, as well as acoustic elements within the space between the speaker and error microphone.

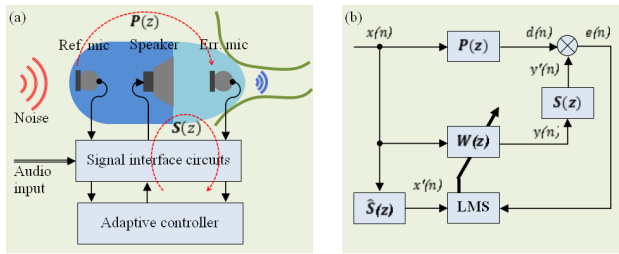


Figure 1. A system overview: (a) ANC integration in earbuds. (b) FxLMS based controller.

In practical implementation, there may be an audio signal feed from the connected device, such as a phone or audio player, that is sent to the speaker. This audio signal could potentially mix with the noise residue measured by the error microphone. However, because information about the audio signal is known, it becomes practical to separate the noise residue. Furthermore, the audio signal can be effectively utilized for both online and offline modeling of the secondary path transfer function^[5]. It is important to note that the scope of this work does not encompass a discussion of the algorithm for separating the noise residue from the audio signal.

The heart of the adaptive controller is a digital filter, generally classified into two major categories: recursive and non-recursive. The former reuses a part of its output as the input, creating a feedback loop that results in a very long impulse response. While a recursive filter has the potential to reduce the computational burden, it comes with inherent drawbacks, such as response instability and local minimum solutions. In this work, the preference is for a non-recursive digital filter to facilitate convergence during adaptation. It consists of one row of unit delays, where a segment of input data is stored, and another row of

coefficient memories of the same length. The output of the digital filter is the sum product of the values in the corresponding rows. Alongside an algorithm for adjusting filter coefficients, an adaptive controller is constructed.

2.1 A review of the FxLMS algorithm

In this work, the least mean square algorithm is considered. The algorithm iteratively adjusts the filter coefficients in a way that minimizes noise residue by following the negative direction of the error gradient. However, the presence of a secondary path causes a phase mismatch in the arrival of the anti-noise signal, impeding the correct filter update. Therefore, an auxiliary filter must be introduced into the control loop to compensate for the alteration of the anti-noise signal by the secondary path^[6]. This auxiliary filter, often referred to as a secondary path estimate, $\hat{S}(z)$, can be obtained through transfer function modeling or measurement. This approach is known as the FxLMS algorithm.

The block diagram in **Figure 1(b)** illustrates an adaptive feed-forward controller, $W(z)$, which is implemented as a non-recursive filter with a length of L . In response to the input, $x(n)$, provided by the reference microphone, the controller generates the anti-noise signal, $y(n)$, which can be calculated using the following relationship,

$$y(n) = \sum_{l=0}^{L-1} w_l(n)x(n-l) = w^T(n)x(n) \quad (1)$$

Here, w_l denotes the l -th coefficient of the controller. The anti-noise signal is transmitted through the speaker to produce,

$$e(n) = d(n) + y'(n) = p^T(n)x(n) + s^T(n)y(n) \quad (2)$$

which is the noise residue measured by the error microphone. This equation uses a positive sign to signify the superposition of sound waves between the unknown ambient noise, $d(n) = p^T(n)x(n)$, and the anti-noise, $y'(n) = s^T(n)y(n)$, as they reach the control point.

The gradient of the error surface can be obtained by differentiating the cost function $J(n) = e^2(n)$ with re-

spect to the filter coefficients. By applying the gradient descent algorithm, the iterative process for adjusting the controller coefficients is expressed as follows,

$$w(n+1) = w(n) - \mu x'(n) e(n) \quad (3)$$

Here, notations μ and $x'(n) = \hat{s}^T(n) x(n)$ represent the iteration step and the filtered reference input, respectively. The iteration step, which is associated with convergence speed, is a positive coefficient that can be selected from a range of values that is not larger than,

$$\mu_{max} = \frac{1}{\|x'(n)\|^2(L + \delta_s)} \quad (4)$$

The notations μ_{max} and δ_s represent the maximum applicable iteration step and the inherent delay in the secondary path, respectively. Accordingly, it is evident that the delay in the secondary path imposes a constraint on convergence speed^[7]. A longer path delay leads to slower convergence.

2.2 The importance of the secondary path

If perfect noise cancellation is achievable, meaning $e(n) \rightarrow 0$ as the adaptation converges, the optimal controller, $W_o(z)$, can be derived from Equation (1) and Equation (2) as:

$$W_o(z) = -\frac{P(z)}{S(z)} \quad (5)$$

To effectively attenuate broadband random noise, the transfer function of the controller, $W(z)$, should closely match the impulse response of the optimal controller. This is achievable if the inverse of $S(z)$ exists. Therefore, it is desirable to have a secondary path that can be represented by a causal and minimum-phase transfer function. In practice, the delay in the secondary path should be shorter than that in the primary path. Additionally, when using a non-recursive filter as the controller, it should have sufficient length to accommodate the rational part of the equation. Fortunately, the control plant associated with this setup is expected to be of low order due to the relatively small acoustical volume within the earbuds.

2.3 Performance factors in noise reduction

The causality condition, which must be satisfied

by any ANC system to allow a broadband noise cancellation, is met when the time required for the anti-noise to be generated and delivered to the control point is faster than the noise propagation time across the primary path. In short, it is fulfilled when the delay in the electrical path is smaller than that in the acoustical path.

The primary contributors to electrical delay include the time required for signal conditioning, data conversion, and computation process. Signal conditioning in the anti-aliasing and reconstruction filters introduces a latency that is proportional to the filter order and inversely proportional to the filter corner frequency. The time for signal conversion between analog and digital domains depends on the type of converter and the number of bits involved. For example, given the same resolution, a Delta Sigma ADC is typically slower than a SAR ADC. Computation in the controller consumes one sample period during which the processor executes an adaptive control algorithm. The latency of the speaker and microphones also contributes to electrical delay.

The delay of the acoustic primary path can be influenced by various factors. In earbuds, device fitting and enclosure provide passive isolation that can increase the delay in the primary path^[8]. Intuitively, acoustic leakage reduces the delay and the lowest estimate of acoustic delay, δ_{act} , can be calculated from the direct sound propagation as follows:

$$\delta_{act} = (\Delta x_{re} - \Delta x_{ye}) / c_0 \quad (6)$$

Here, Δx_{re} represents the distance between the two microphones, Δx_{ye} represents the distance between the speaker and the error microphone, and c_0 is the sound speed, approximately 343 m/s. However, when the path of arriving noise is closer to the error microphone than the reference microphone, the acoustic delay may not be sufficient to ensure causality^[9]. This condition is purely physical and is less related to the allocated filter length in the controller. Practical remedies include increasing the acoustic path delay by improving passive isolation and enhancing spatial information using the multi-reference microphone method. The sound passing through the earbuds enclosure and ear-tip can improve the

performance of the feedforward system by increasing the delay between the two microphones^[10]. The use of additional reference microphones provides a comprehensive representation of noise coming from various directions^[11].

Coherence in measurements defines the noise reduction performance of an ANC system because the adaptation of controller coefficients relies on two correlated pieces of information provided by the error microphone and reference microphone. Based on the analysis of random processes, the noise reduction, θ , at a given frequency ω can be estimated as:

$$R(\omega) = 10 \log_{10} (1 - \gamma_{xe}^2(\omega)) \text{ dB}$$

where $\gamma_{xe}^2(\omega)$ represents the coherence function between the output of the reference microphone and the output of the error microphone when the ANC system is inactive^[12]. The coherence function has a range of values between 0 and 1, indicating the quality of signal coherence, from poor to excellent. This can be interpreted as follows: The higher the coherence between the signals provided by the microphones, the greater the noise reduction to be expected. In practice, signal coherence is primarily affected by the quality of the instrumentation system, such as microphone dynamic range, sensitivity, and directivity, as well as distortion in the signal amplification unit. Additionally, cable shielding and circuit isolation can help minimize input contamination from signal interference.

In addition to its impact on system latency, the proper positioning of the speaker and microphones is crucial for controllability. While the enclosure of earbuds is the obvious place for a speaker, the opening of the ear tip can extend beyond the ear canal open end, creating an impedance mismatch where sound waves are transmitted and reflected. Conceptually, the optimal position for the speaker is at the dominant anti-node. In terms of the reference microphone position, controller complexity can be reduced if the microphone picks up a negligible amount of the anti-noise radiated from the speaker. Therefore, it is desirable to block the acoustic feedback path through proper enclosure design. As for the error micro-

phone, the ideal location is near the speaker, where the noise residue is present with a high correlation to the reference noise.

The performance of the controller is intricately linked to numerical accuracy, which, in turn, is dependent on the choice between floating-point and fixed-point systems in the processing hardware^[13]. Floating-point systems offer the advantage of high precision, making them well-suited for applications where numerical accuracy is critical. However, typically demanding more computational resources can strain the limited processing capabilities of devices like earbuds. On the other hand, fixed-point systems, while more resource-efficient, may introduce numerical errors due to lower precision, which can potentially impact the accuracy of controller operations. The causes of numerical error in fixed-point systems are primarily related to the limited number of bits available for representing numbers and rounding during arithmetic operations. To address these errors, careful consideration of scaling, quantization, and rounding techniques can be employed in fixed-point implementations to enhance the accuracy of controller calculations.

3. Implementation of adaptive ANC

Developing high-performance noise-canceling earbuds involves considering numerous aspects^[14], such as the comprehensive acoustic design to produce favorable characteristics in the earbuds, which significantly impacts noise cancellation performance. Earbuds for ANC applications require careful integration of components such as speakers, microphones, controllers, and partitions. The arrangement of these components within a compact, well-shaped enclosure defines the interaction between noise and anti-noise. Additionally, it is crucial to incorporate low-latency electroacoustic components into the system.

While the design of the earbuds is a critical factor, this study does not cover every aspect of creating the perfect earbuds. It primarily focuses on realizing the adaptive controller. Therefore, for the experimentation, earbuds sourced from the Bose QC30 are used.

Originally, these components were connected to the main board in the neckband via cables. Each unit of the earbuds has approximate dimensions of $28 \times 30 \times 20$ mm and is equipped with two 4 mm electret microphones and one 15 mm speaker with an impedance of 32Ω . To gain access to the internal parts, a few modifications were made: the earbuds need to be separated from the main board and the connecting cables must be traced to identify the internal parts.

Two compartments can be found within the earbuds. The first one houses the error microphone and the speaker, facing inward toward the ear tunnel. It is isolated from the second compartment where the reference microphone is set. The reference microphone is facing outward to pick up ambient noise entering the ear. The distance between the reference microphone and the error microphone and the distance between the speaker and the error microphone is 8.5 mm and 2 mm, respectively, resulting in an acoustic delay of approximately $19 \mu\text{s}$ in this setup.

High-performance DSP is essential for controller development in ANC applications, particularly for earbuds. However, implementing ANC in earbuds can have a significant impact on device operation time. In short, the DSP should be compact, require minimal components to support its operation, energy-efficient, and cost-effective. These qualifications hold especially true when considering processor choices for mid and upper-range commercial earbuds. For example, options like the Qualcomm S5 Sound Platform and the Apple H2 BT5.3 Audio-SoC offer functionality for audio processing, voice services, and device connectivity in a single SoC component, all while operating with low power consumption.

For performing general experimentation, several commercial DSP options with the corresponding development boards are available, including the CS47L85, i.MX RT1020, and TMS320C5517. Concerning the computational speed, it must ensure that the delay in the electrical path is shorter than in the acoustical path. Theoretically, assuming a $19 \mu\text{s}$ acoustic delay, any DSP working at a sample rate of 96 kHz or higher is sufficient. A minimum of two in-

put channels and one output channel are required. In this study, the evaluation board EVAL-ADAU1787Z from Analog Devices, depicted in **Figure 2(a)**, is employed. This choice aligns with the study objectives as it addresses the challenge posed by the limitation of computational resources. Additionally, the small DSP footprint makes it a practical choice for integration into earbuds.

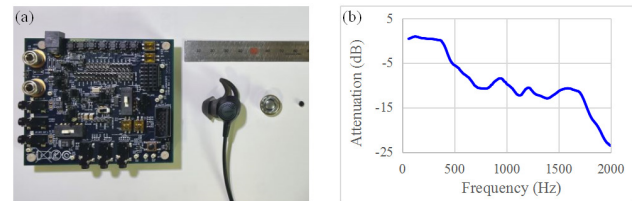


Figure 2. Device selection: (a) DSP board and earbuds. (b) Passive noise isolation in earbuds.

The evaluation board is equipped with four ADC channels, two DAC channels, a low-power audio codec, and two fixed-point DSP cores. The first core is the FastDSP audio processing engine, offering built-in features such as biquad filters, signal limiters, mixers, and volume controls. When passing a signal from the ADC input to the DAC output at a sampling frequency of 768 kHz, a group delay of $5 \mu\text{s}$ can be expected^[15]. This particular core can be programmed to perform specific tasks using no more than 64 instruction cycles. Here, group delay represents the time shift of a packet of oscillating waves centered around one frequency that travels together. An instruction cycle denotes a discrete step a processor takes to execute a single machine-level instruction.

The second core in the processor is the 28-bit SigmaDSP audio processing core, offering additional built-in functions, including FIR filters and many custom algorithms. For this particular core, the maximum number of instruction cycles varies depending on the sampling frequency, ranging from 32 instructions at 768 kHz to 512 instructions at 48 kHz. Moreover, the core supports a high-performance mode achieved by overclocking, which doubles the number of available instruction cycles. It is worth to note the aforementioned active noise algorithm is implemented here using one DSP core, which is, the SigmaDSP core at the normal clock mode.

3.1 Software development tool

For programming the SigmaDSP product lineup, Analog Devices provides SigmaStudio, which is a graphical programming environment for creating and deploying signal processing programs on the evaluation board. It comprises two fundamental frameworks, the first one offers access at the DSP register level to assign built-in operational features, including power management, signal conditioning filters, data interpolation and decimation, and channel routing between input and output (I/O) ports and the DSP cores.

The second framework involves schematic tools that allow the assembly of functional blocks to perform signal manipulation and control. These composed schematics establish operational flow in the device, which is called repeatedly at the start of each sampling period. Each schematic block consumes computational resources in terms of instruction cycles and memory usage. Given the limited instruction capacity at high sampling frequencies, it is crucial to know the minimum feasible sampling frequency and utilize computationally efficient blocks accordingly. Fortunately, memory resources are relatively abundant.

There are scenarios where essential schematic blocks for ANC applications cannot be used due to their high instruction cycle demands. For instance, the built-in L -tap FIR filter function consumes 13 instruction cycles for function overhead and $L + 8$ instruction cycles for sub-routine overhead. Moreover, modifying the filter coefficients during program execution is also not feasible. Therefore, to implement an efficient ANC program, it becomes necessary to employ custom code that grants access to low-level functionality such as shift registers, multiply and accumulate (MAC) operations, as well as the memory read and the memory write operations. With custom code, an L -tap FIR filtering can be accomplished in L cycles of MAC instructions and 1 cycle of memory transfer. The shifting of filter data is automatically managed in the shift register at the start of each sampling period. Detailed discussions of low-level programming are beyond the scope of this article.

3.2 Design of the controller

A reasonable target performance of the controller must be defined, such as the desired minimum noise attenuation within a given bandwidth. One way to determine these parameters is by assessing the passive noise isolation provided by the earbuds. To evaluate this, measurement was conducted in a controlled listening environment using an artificial head and torso (HEAD Acoustic HTB V) with a loudspeaker as the sound source. The loudspeaker was positioned one meter in front of the ear. A broadband, uniformly distributed random noise served as the excitation signal. By comparing the internal microphone responses with and without the earbuds attached to the ears, the passive noise isolation plot displayed in **Figure 2(b)** was obtained. From the data, one may say the passive noise attenuation below 750 Hz is poor. Therefore, the target to achieve in this work is a significant noise reduction of at least 10 dB in the operating bandwidth extending up to 1 kHz.

Considering that the earbuds are sourced from an external commercial product and cannot be modified, it is crucial to ensure the system is causal. To do this, initial data about acoustic paths in the earbuds was collected through measurements using the mentioned test equipment. A sine-sweep signal served as the excitation source. In the primary path measurement, the signal was directed towards an external loudspeaker, and the impulse response function between the two microphones was recorded. In the case of the secondary path, the signal was directed to the speaker in the earbuds, and the path response was captured from the DSP output port, which is directly connected to the earbuds error microphone.

Taking into account the assumed 19 μ s acoustic delay, the DSP sampling rate option that meets the minimum requirement is 96 kHz. The measurement results at this specific sampling frequency are depicted in **Figure 3(a)**. One can notice that the leading peak in the impulse response function of the primary path exhibits a lower amplitude compared to the secondary path, which is expected due to higher path attenuation. It is worth noting that the first peak in the primary path impulse response follows that of

the secondary path, indicating the system is causal. In conclusion, the arrangement of microphones and the speaker within the earbuds, along with the choice selection of a 96 kHz DSP sampling rate, confirms system causality.

Based on the initial assessment, the programming work for creating the adaptive feedforward controller can begin. Running at 96 kHz, the SigmaDSP core at its normal clock rate can handle a maximum of 256 instruction cycles. Approximately 43 instruction cycles are reserved for core housekeeping. This means the entire algorithm, along with I/O port assignments, must fit within a total of 213 instruction cycles. The bare minimum noise cancellation program comprises built-in functions and custom code. The built-in functions handle essential tasks such as ADC input, signal generator, two-state logic switching, and DAC output. On the other hand, the custom functions are responsible for signal conditioning in the upstream path, reference input filtering, and adaptive control. After allocating computational resources to the built-in functions, 200 instruction cycles remain available for reference input filtering and adaptive control. It is important to optimize the filter lengths for these functions to ensure efficient use of this allocated resource.

There are three functional blocks in the FxLMS algorithm that handle: anti-noise calculation, as represented by Equation (1), reference input filtering, and coefficient adaptation following Equation (3). The first two blocks, essentially filters, consume one

instruction cycle per filter coefficient, while the last block consumes three instruction cycles per filter coefficient. **Table 1** provides a summary of the distribution of instruction allocations for three potential design scenarios. In the first column, the controller and the secondary path estimates are non-recursive filters. Referring to **Figure 3(a)**, it is evident that a substantial filter length is required when using a non-recursive filter to represent the secondary path estimate, approximately 100 taps to cover the first microsecond. This condition restricts the length of the controller to no more than 25 coefficients.

The second scenario involves using a recursive filter to model the secondary path estimate, which has proven advantageous as it significantly reduces the required filter length without compromising controller stability. The optimal filter length for the secondary path estimate is determined using the line search method, which is 16 coefficients in the feed-forward part and 19 coefficients in the feedback part. **Figure 3(b)** provides a comparison between the impulse response functions of the measured the secondary path and secondary path estimate. The length of the controller is significantly expanded to 40 coefficients.

The optimal controller can be used to determine an appropriate controller length. **Figure 4(a)** displays an estimate of the impulse response function of the optimal controller. This calculation, performed without regularization, utilizes the measured acoustic paths. Although not entirely precise, this estimate

Table 1. Basic computational requirements for various programming schemes.

Computation process	Computation cost (instruction cycle)			Notes
	FxLMS ^(a)	FxLMS ^(b)	FuLMS ^(c)	
Core housekeeping	43	43	43	(a). $W(z)$ and $\hat{s}(z)$ are non recursive filters
ADC: Reference signal	2	2	2	
ADC: Error signal	2	2	2	
DAC: Control signal	2	2	2	(b). $W(z)$ is non recursive filter, $\hat{s}(z)$ is recursive filter
Controller output	$LWB + 1$	$LWB + 1$	$(LWB + LWA) + 1$	
Filtering of input	$SWB + 1$	$(SWB + SWA) + 1$	$(SWB + SWA) + 1$	(c). $W(z)$ and $\hat{s}(z)$ are Recursive filters
Filtering of output	-	-	$(SWB + SWA) + 1$	
Controller adaptation	$2 + 3 LWB$	$2 + 3 LW$	$4 + 3(SWB + SWA)$	

serves as an initial approximation for determining the required length of the controller filter. It becomes evident that the first microsecond of the impulse response function carries over 90% of the signal power. While it is conceivable to set the controller length near 100 to mimic the dominant optimal response, this proves unrealistic because the remaining resources support only 40 coefficients.

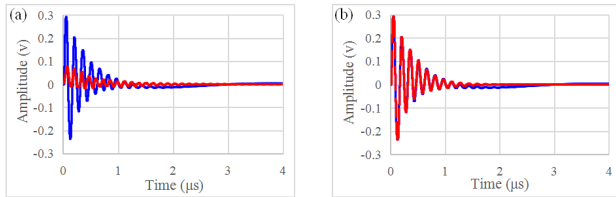


Figure 3. The modeling of secondary paths: (a) The measured impulse response functions of the earbud’s primary path (red) and secondary path (blue). (b) Comparison between impulse response functions of the measured (blue) and the modeled (red, dashed) secondary paths.

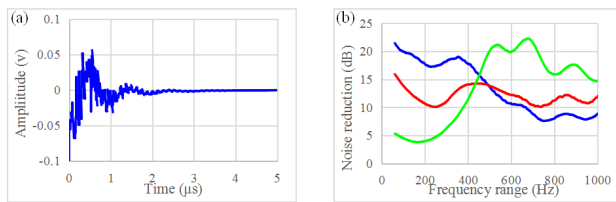


Figure 4. Design of the controller: (a) A non-regularized impulse response function of the optimal controller estimate. (b) The performance of the controller in terms of noise reduction at a given multi-rate factor $N_d = n$ (green), $N_d = 2n$ (red), $N_d = 4n$ (blue).

While one may suggest an alternative approach involving a recursive filter as the controller, it is essential to note that, as detailed in the third column of **Table 1**, additional resources must be allocated for output filtering during the adaptation of the feedback filter. The feedback loop may potentially put controller stability at risk during adaptation. Nevertheless, there is some potential, considering recent developments in alternative algorithms that aim to address stability^[16]. Another suggestion, applied here, is based on multi-rate signal processing^[17]. It is a straightforward approach that involves decimating the signals. The processes for filter adaptation and anti-noise generation are performed at different rates.

In summary, the final configuration is as follows: a 40-tap non-recursive filter for the controller and a

35-tap recursive filter as the secondary path estimate, which corresponds to a total of 248 instruction cycles. A few more instruction cycles were allocated for a second-order recursive filter, inserted upstream for input signal treatment. The performance of the controller to cancel broadband random noise is depicted in **Figure 4(b)**. Interestingly, the slopes of the plots at different multi-rate factors, denoted as N_d , show variations around 450 Hz. It is believed that with a smaller multi-rate factor, the observation time in the controller becomes shorter, making it challenging for the controller to regulate the low-frequency components, and vice versa. When N_d is set to $2n$, an average noise reduction exceeding 10 dB is achieved in the frequency range up to 1 kHz, satisfies the given design target.

The experimentation showcases adaptive controller design by limiting DSP capability. Greater noise reduction over a wider frequency range becomes attainable with additional resources. For instance, running the DSP board in overclock mode doubles the total instruction cycles to 512. Furthermore, utilizing Biquad filters in the FDSP core to model the secondary path estimate frees up more instruction cycles. Some signal processing functions, such as multi-rate signal processing, are performable by the hardware. These additional resources offer the feasibility of expanding controller length and implementing sophisticated algorithms for improved noise cancellation.

4. Conclusions

The study discussing the development of active noise control systems for earbuds has been presented, emphasizing the significance of maintaining low latency to ensure causality for effective broadband noise cancellation. Nevertheless, when working within the constraints of earbuds, the available hardware resources are limited, hindering the utilization of sophisticated adaptive control algorithms. To overcome these limitations, optimization of filter configuration is employed, along with implementing a computationally efficient program. Moreover, multi-rate signal processing techniques provide practical solutions for achieving the desired noise reduction.

Conflict of Interest

I declare that there is no conflict of interest regarding the publication of this paper.

Funding

This research received no external funding.

Acknowledgement

The author extends gratitude to Dr. Ji-Ho Chang of the Korea Research Institute of Standards and Science, Daejeon, and Prof. Sung-Hwan Shin of Kookmin University, Seoul, for providing access to the test facility and experimental equipment.

References

- [1] Liebich, S., Fabry, J., Jax, P., et al. (editors), 2018. Signal processing challenges for active noise cancellation headphones. *Speech Communication; 13th ITG-Symposium; 2018 Oct 10-12; Oldenburg. Berlin: VDE.* p. 1-5.
- [2] Bai, M., Lee, D., 1997. Implementation of an active headset by using the H_{∞} robust control theory. *The Journal of the Acoustical Society of America.* 102(4), 2184-2190.
- [3] Goldstein, A.L. (inventor), 2016. Adaptive feedback control for earbuds headphones and handset. Patent Application Publication. US patent. 2016/0300562 A1.
- [4] Kim, Y., Park, Y., 2019. CPU-GPU architecture for active noise control. *Applied Acoustics.* 153, 1-13.
- [5] Gan, W.S., Kuo, S.M., 2002. An integrated audio and active noise control headset. *IEEE Transactions on Consumer Electronics.* 48(2), 242-247.
- [6] Morgan, D., 1980. An analysis of multiple correlation cancellation loops with a filter in the auxiliary path. *IEEE Transactions on Acoustics, Speech, and Signal Processing.* 28(4), 454-467.
- [7] Kuo, S.M., Morgan, D.R. (editors), 2000. Review of DSP algorithms for active noise control. *IEEE International Conference on Control Applications. Conference Proceedings (Cat. No. 00CH37162); 2000 Sep 27; Anchorage. New York: IEEE.* p. 243-248.
- [8] Zhong, X., Zhang, D., 2021. Latency prediction of earmuff using a lumped parameter model. *Applied Acoustics.* 176, 107870.
- [9] Zhang, L., Qiu, X., 2014. Causality study on a feedforward active noise control headset with different noise coming directions in free field. *Applied Acoustics.* 80, 36-44.
- [10] Rafaely, B., Jones, M., 2002. Combined feedback—feedforward active noise-reducing headset—The effect of the acoustics on broadband performance. *The Journal of the Acoustical Society of America.* 112(3), 981-989.
- [11] Iwai, K., Kinoshita, S., Kajikawa, Y., 2019. Multichannel feedforward active noise control system combined with noise source separation by microphone arrays. *Journal of Sound and Vibration.* 453, 151-173.
- [12] Hansen, C., Snyder, S., Qiu, X., et al., 2012. Active control of noise and vibration. CRC Press: Boca Raton.
- [13] Chang, C.Y., 2009. Efficient active noise controller using a fixed-point DSP. *Signal Processing.* 89(5), 843-850.
- [14] Huang, C.H., Pawar, S.J., Hong, Z.J., et al., 2012. Earbud-type earphone modeling and measurement by head and torso simulator. *Applied Acoustics.* 73(5), 461-469.
- [15] Four ADC, Two DAC, Low Power Codec with Audio DSPs ADAU1787 [Internet]. Analog Devices; 2020. Available from: <https://www.analog.com/media/en/technical-documentation/data-sheets/adau1787.pdf>
- [16] Mohammed, J.R., Singh, G. (editors), 2007. An efficient RLS algorithm for output-error adaptive IIR filtering and its application to acoustic echo cancellation. *2007 IEEE Symposium on Computational Intelligence in Image and Signal Processing; 2007 Apr 1-5; Honolulu. New York: IEEE.* p. 139-145.
- [17] Graf, J., Reithmeier, E., 2009. Computationally efficient active noise reduction in headsets. *Journal of Computer and Systems Sciences International.* 48, 567-573.